Analytical Equation of State for Solid-Liquid-Vapor Phases[1]

A. Yokozeki[2]

A simple analytical equation of state has been proposed for describing the phase behavior of three thermodynamic states (solid, liquid, and vapor) of matter. In terms of reduced parameters, it can be written as:

$$P_r = \frac{T_r}{V_R - b_R}\left(\frac{V_R - d_R}{V_R - c_R}\right) - \frac{a_R}{V_R^2}.$$

P_r and T_r are reduced pressure and temperature with respect to the critical pressure (P_c) and temperature (T_c), respectively, while V_R is a reduced molar volume defined as $V_R = P_c V / R T_c$, where R is the universal gas constant. This may be regarded as an extension of the classical van der Waals's equation of state for fluid (liquid and vapor) only states. The four parameters, a_R, b_R, c_R, and d_R in this equation are free adjustable constants, and can be variable with temperature. The basic physical idea underlining the model is presented, and examples applied successfully to actual pure substances and mixtures are demonstrated. Also, applications to the hard-sphere model are examined. Further improvements, limitations, and possible applications of the present model are discussed.

KEY WORDS: argon; carbon dioxide; equation of state; liquid; methane; phase equilibria; solid; vapor.

1. INTRODUCTION

In 1873, van der Waals proposed an empirical equation of state (EOS) in his doctoral dissertation [1] in order to describe the phase behavior of fluids (gas and liquid states). It has been an epoch-making equation,

---

although the derived equation was originally based on a rather intuitive idea and limited experimental observations. His contribution on the unified view of gas and liquid states was properly acknowledged with the Nobel Prize in Physics in 1910. Later, his intuition and insight have been proved to be theoretically correct under physically reasonable assumptions. The equation is composed of a hard-core repulsive part, P_{HC} and an intermolecular attractive part, P_A:

$$P = P_{HC} + P_A = \frac{RT}{V-b} - \frac{a}{V^2}. \tag{1}$$

The validity of the separation of P_{HC} and P_A, as well as the phase transition behavior, has been rigorously proved by Lebowitz and Penrose [2]. This simple-looking EOS predicts essentially all fluid phase behaviors of classical fluids correctly, at least in a qualitative way. It is not only valid for pure fluid behaviors, but also for mixtures. Among others, one of the most striking predictions for mixture properties may be the topological classification of the global fluid-phase diagram of binary mixtures made by van Konynenberg and Scott [3].

Since the celebrated van der Waals EOS, numerous modified van der Waals EOS have been proposed to improve the numerical accuracy [4], and are categorically called a general "cubic" EOS, because they can be written in terms of a cubic polynomial equation of molar volume, V. Typical modifications may be written as:

$$P = \frac{RT}{V-b} - \frac{a}{V^2 + qbV + rb^2}. \tag{2}$$

For example, if $q = r = 0$, it is the original van der Waals EOS, if $q = 1$ and $r = 0$ with $a = 1/\sqrt{T}$, it is the Redlich–Kwong EOS [5], if $q = 2$ and $r = -1$ with a general T-dependence of a, it is called a Peng–Robinson type EOS [6], and so on. Sometimes the b parameter is allowed to be a function of T as well, in order to represent real fluid properties more accurately. These modified cubic EOS have been found to be quite useful in the actual application of engineering processes [4, 7].

Further improvement for the van der Waals EOS has been a modification of the first term of Eq. (1): the repulsive part of EOS, P_{HC}. Among others, the most popular version of this modification is due to Carnahan and Starling [8]. They have proposed the empirical form,

$$P_{HC} = \frac{RT}{V} \frac{1 + \eta + \eta^2 - \eta^3}{(1-\eta)^3}, \qquad \eta \equiv \frac{b}{4V}, \tag{3}$$

which agrees very well with the *fluid branch* of computer simulations of hard-sphere assemblies and also is in good agreement with the theoretical Percus–Yevick hard-sphere isotherms [9]. Extensive applications with this modification have been reported in the literature [10, 11]. The volumetric, particularly liquid-phase, properties, have been significantly improved numerically, but no qualitatively new predictions have resulted.

All these equations and more sophisticated fluid EOS are able to predict VLE (vapor-liquid equilibria), LLE (liquid-liquid equilibria), VLLE (vapor-liquid-liquid equilibria), and critical points of VLE and LLE as well as all other thermodynamic properties, *except for* the phase behaviors and thermodynamic properties including the solid state. In practice, the solid state is usually treated as a separate and different thermodynamic equation at the phase transition, and then the phase equilibrium is solved by combining the fluid-phase EOS [12].

The first attempt to include the solid state in a unified equation of state was made by Longuet–Higgins and Widom [13]. They adopted the numerical data from the computer "experiments" of hard spheres [14] for the P_{HC} part in the wan der Waals EOS, and calculated the thermodynamic properties at the SLV (solid-liquid-vapor) triple point of argon with some reasonable assumptions. Later, with the advent of powerful computers, systems having more realistic interaction potentials were investigated in order to simulate the SLV behavior using Monte Carlo computations. Hansen and Verlet [15] used the Lennard-Jones potential and applied the model to argon's SLV phase behavior, while Hiwatari and Matsuda [16] employed a more general [Kac] potential to predict melting properties of noble gases and alkali metals and called their model "Ideal Three-Phase Model." Very recently, Lamm and Hall [17] have made Monte Carlo computer experiments to construct the SLV three-phase diagrams for binary Lennard-Jones mixtures.

However, to our best knowledge, only few algebraic equations, quantitatively describing solid-liquid-vapor phases, have been reported in the literature [18–20]. The purpose of the present work has been to develop such an EOS. In this report, we propose a simple analytic EOS describing the SLV behavior in a unified way, and it can be regarded as an extension of the van der Waals fluid EOS. First, the basic physical idea underlying our model is presented. Then the method to set up the proper EOS parameters is discussed for the practical application. In Section 3, we apply the present EOS to actual pure substances: argon, methane, and carbon dioxide. Then, the application to mixtures is examined using a binary system of carbon dioxide/methane mixtures. Also, the well-known solid/fluid phase transition of hard-sphere ensembles is analyzed with this algebraic EOS. In Section 4, discussions of the present analyses, further

improvements and limitations of the EOS, and possible useful applications are given, and then concluding remarks follow.

2. MODEL DEVELOPMENT

The thermodynamic principles [the zeroth and first laws] prove the existence of an EOS, a functional form among T, P, and V variables in an equilibrium state, although the specific form cannot be predicted. In general, the form of the EOS is necessarily empirical, except for the ideal gas EOS and certain statistical mechanical models. However, the functional form cannot be arbitrary, but must satisfy empirically known facts. Among others, the EOS properties of pure substances, important and relevant to the present model development are:

(a) When $V \to \infty$, it will approach the ideal gas form: $PV = RT$.

(b) The thermodynamically stable state, including metastable states, must satisfy the mechanical stability condition of $(\frac{\partial P}{\partial V})_T \leqslant 0$.

(c) The existence of the vapor-liquid critical point.

(d) The existence of the stable solid phase, which has a liquid-like steep slope in $(\frac{\partial P}{\partial V})_T$, having a region with $P > 0$, in addition to the liquid and vapor phases.

(e) There exists no critical point between solid and fluid equilibria.

(f) The existence of the first-order phase transition between vapor and liquid (VLE), solid and liquid (SLE), and solid and vapor (SVE), where the so-called van der Waals "S" loop exists in the isothermal PV diagram, and the Maxwell's equal-area construction can be applied over the "S" loop.

(g) The existence of negative pressure regions and the condition of $(\frac{\partial P}{\partial V})_T > 0$ are allowed within the "S" loop.

Then we look for a simple analytical EOS which satisfies these conditions. Equation (1), or a more general form, Eq. (2), certainly satisfies these conditions *except for the solid state*, since it does not possess the "solid-phase branch" in the physically valid region: $V > b$. One might consider a fifth-order (or higher-order) polynomial form in V, which could possess an additional continuous van der Waals "S" loop in the PV diagram, presenting the solid-liquid phase transition, besides the vapor-liquid transition "S" loop. This is certainly possible. However, such an analytically continuous function leads to the existence of a solid-fluid critical point, not satisfying the required condition (e). Thus, the solid-phase branch in an EOS must be separated from the fluid-phase branches and analytically discontinuous at

solid-fluid transitions. Then algebraic and topological arguments, which satisfy the conditions (a) through (g), lead to an EOS expression of the following form, as being an extension of the van der Waals *fluid* EOS:

$$P = \frac{RT}{V-b}\left(\frac{V-d}{V-c}\right)^k - \frac{a}{V^2 + qbV + rb^2}, \tag{4}$$

where constants $a, b, c,$ and d are all positive numbers with $b < d < c$, $k = $ integer, the physically valid region of EOS is $V > b$, and q and r have the same meanings as those in Eq. (2). This form has been inspired from considerations of the analytical and topological geometry. It may be best appreciated by schematic isotherms in the PV diagram illustrated in Figs. 1 and 2 at the SLV (solid-liquid-vapor) triple point, where the constants a, b, c, d, q, and r are assumed to be "proper" values to produce such desired EOS. Both cases of $k = $ odd and even integers possess physically acceptable shapes, although the topology in the solid branch is different. These figures are easily constructed without performing numerical calculations, using the fact that at $V = b$ or c, $P_{HC} \to \pm\infty$, (the sign depends upon the relative order among b, c, and d as well as the parity of $k = $ odd or even); $P \to 0$ at
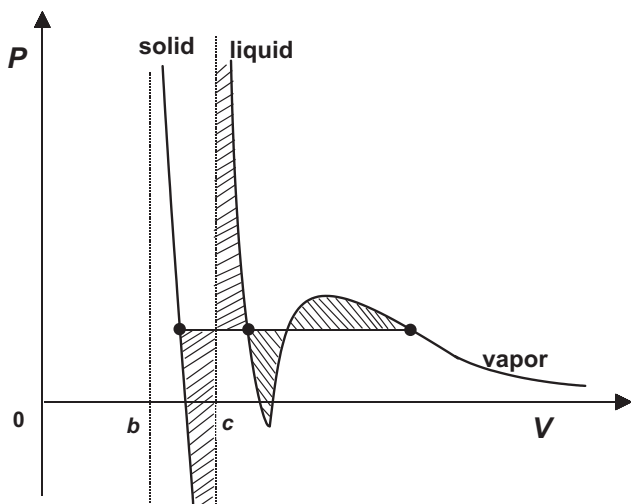
Fig. 1. Schematic isothermal PV diagram of Eq. (4) with $k = $ odd integer at the solid-liquid-vapor triple point: $0 < b < d < c$ and $V > b$. The hatched areas are the Maxwell's equal area construction, and the solid circles are the equilibrium points for the solid, liquid, and vapor phases.

$V \to \infty$; when $V = d$, $P_{HC} = 0$; P is the sum of two functions, P_{HC} and P_A, P_A is the familiar van der Waals attraction part, and the total number of roots of the polynomial equation, Eq. (4) is known.

The regions with $dP/dV > 0$ are of course thermodynamically unstable, being similar to the case of the van der Waals EOS within the "S" loop. It should be noted that the solid and liquid branches do not possess the ordinary van der Waals continuous "S" loop, but here the "S" loop forms an "infinite-size S" loop. This is because $P \to \pm\infty$ at $V = c$. However, as far as the phase equilibrium is concerned, it is not fundamentally different from the "ordinary continuous finite-size S" loop. The equilibrium condition can be equally applied with Maxwell's equal-area construction for the two (α and β) phase equilibrium over the "S" loop, mathematically $P(V_\alpha - V_\beta) = \int_{V_\beta}^{V_\alpha} P \, dV$, as long as the integral has a finite value. However, the important difference is that this "infinite-size S" loop does not lead to any solid-liquid critical point. Thus, the EOS condition (e) is satisfied.

Equation (4) with a general k value becomes complicated when we derive various thermodynamic relations and properties, although they can be written in analytically closed forms. Since the qualitative predictions
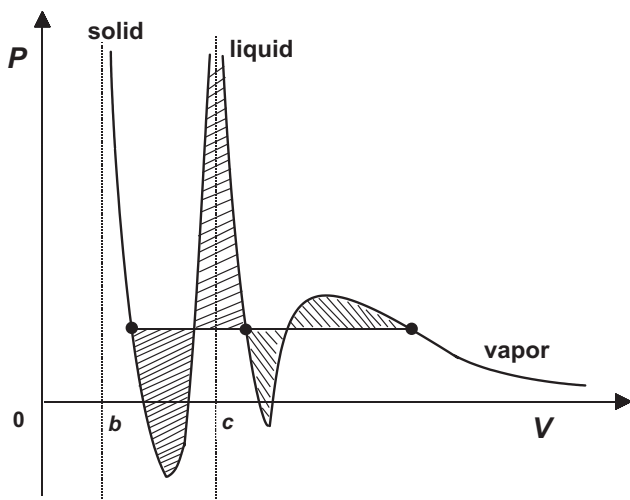
Fig. 2. Schematic isothermal PV diagram of Eq. (4) with $k =$ even integer at the solid-liquid-vapor triple point: $0 < b < d < c$ and $V > b$. The hatched areas are the Maxwell's equal area construction, and the solid circles are the equilibrium points for the solid, liquid, and vapor phases.

based on these general-k EOS are expected to be the same, we choose the simplest case, that is, $k = 1$ and also $q = r = 0$. In the following analysis, we examine this type of EOS:

$$P = \frac{RT}{V-b}\left(\frac{V-d}{V-c}\right) - \frac{a}{V^2}. \tag{5}$$

In terms of dimensionless parameters, it can be written as:

$$P_r = \frac{T_r}{Z_c(V_r - b_r)}\left(\frac{V_r - d_r}{V_r - c_r}\right) - \frac{a_r}{V_r^2 Z_c^2}, \tag{6}$$

where the reduced parameters are defined:

$$Z_c = \frac{P_c V_c}{RT_c}, \qquad P_r = \frac{P}{P_c}, \qquad T_r = \frac{T}{T_c}, \qquad V_r = \frac{V}{V_c} \tag{7}$$

$$b_r = \frac{b}{V_c}, \qquad c_r = \frac{c}{V_c}, \qquad d_r = \frac{d}{V_c} \tag{8}$$

$$a_r = \frac{P_c a}{(RT_c)^2}. \tag{9}$$

Then the compressibility factor, Z becomes:

$$Z = Z_c \frac{P_r V_r}{T_r} = \frac{V_r}{V_r - b_r}\left(\frac{V_r - d_r}{V_r - c_r}\right) - \frac{a_r}{V_r Z_c T_r}. \tag{10}$$

A more compact dimensionless form of Eq. (5) is:

$$P_r = \frac{T_r}{V_R - b_R}\left(\frac{V_R - d_R}{V_R - c_R}\right) - \frac{a_R}{V_R^2}, \tag{11}$$

where the volumetric parameters are reduced by a factor of P_c/RT_c, instead of the critical volume V_c: $V_R = \frac{P_c V}{RT_c} = Z_c V_r$, $b_R = \frac{P_c b}{RT_c}$, $c_R = \frac{P_c c}{RT_c}$, $d_R = \frac{P_c d}{RT_c}$, and $a_R = a_r$.

The qualitative EOS shape such as shown in Figs. 1 and 2 is easily constructed by use of the elementary knowledge of analytical geometry, without making any numerical analyses. However, to set up proper constants for a, b, c, and d in the present EOS requires some numerical analyses. Often, the critical-point conditions, $dP/dV = d^2P/dV^2 = 0$, are employed to determine the constants of a simple EOS, such as a general cubic EOS, Eq. (2). This method determines a maximum of three constants, since the conditions provide only three independent coupled equations.

Here, four parameters cannot be uniquely determined, but the existence of the critical point in an EOS provides necessary constraints among these four parameters. Using the reduced EOS form, Eq. (6), the required constraints for the existence of the critical point are derived as:

$$3a_r b_r c_r / Z_c^2 - b_r c_r - d_r / Z_c - a_r / Z_c^2 + 3 = 0 \tag{12}$$

$$3a_r b_r c_r / Z_c^2 - a_r (b_r + c_r) / Z_c^2 + 1 = 0 \tag{13}$$

$$a_r b_r c_r / Z_c^2 - b_r - c_r - 1/Z_c + 3 = 0. \tag{14}$$

These three equations contain five free parameters, including Z_c. Here, we treat Z_c as an adjustable parameter, or an EOS formal constant, instead of assigning the actual experimental value. This treatment is the same as the common practice in the general cubic EOS, Eq. (2) application [4]. Then, if any two among five parameters are given, the other three parameters are uniquely determined. For example, if b_r and Z_c are specified, c_r is a positive root of the following quadratic equation, derived from Eqs. (13) and (14), when $b_r \neq 1/3$.

$$c_r^2 + c_r (b_r - 3 + 1/Z_c) - b_r (b_r - 3 + 1/Z_c)/(3b_r - 1) = 0 \tag{15}$$

Then, a_r is determined from Eq. (14), and next d_r can be obtained from Eq. (12). In the special case of $b_r = 1/3$, Eqs. (12) to (14) reduce Eq. (6) to the original van der Waals EOS with $Z_c = 3/8$, $a_r = 27/64$, and $c_r = d_r = 0$. The choice of b_r and Z_c, as the two specified parameters, is arbitrary. However, they are convenient for assigning proper values, since they have some physical meanings; i.e., b_r (or equivalently c_r) is a limiting value for the solid (or liquid) reduced volume, and Z_c is the familiar critical compressibility factor. It should be noted that b_r is equivalent (or symmetric) with c_r in the present case ($k = 1$), as clearly seen in Eq. (6). Here we designate the smaller value as b_r, without loss of generality.

Figure 3 shows a summary chart of the numerical and analytical analyses for the proper choice for b_r (or equivalently c_r) and Z_c parameters. Depending upon a set of the parameters, seven topologically different shapes of EOS arise. Regions denoted as **A** in Fig. 3 are the proper parameter region, which corresponds to the EOS type in Fig. 1; i.e., a physically stable solid-phase branch and VLE (vapor-liquid-equilibrium) critical point can exist. The parameter d_r is always between b_r and c_r in this case. In Regions **B** and **D**, the critical point occurs in the solid-phase branch and, for the latter, no stable liquid-phase branch exists. Region **C** has the critical point in the fluid-phase branch, but essentially no stable liquid phase can exist. Region **E** has a proper fluid EOS type, but does not
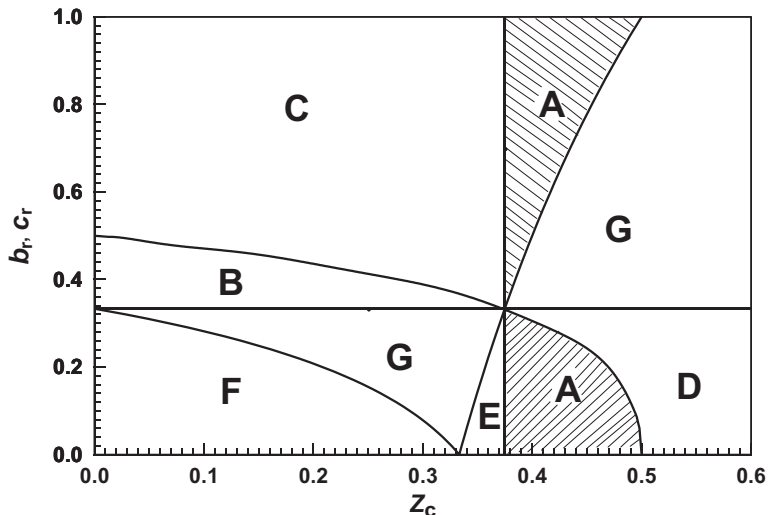
Fig. 3. Classification chart of various topological shapes in Eq. (6). The area denoted **A** is the proper EOS parameter region, which gives physically correct isotherms as illustrated in Fig. 1. See text for other possible shapes, denoted as **B** through **F**. The horizontal line is at $1/3$ and the vertical line is at 0.375.

have a physically meaningful solid-phase branch. In Region **F**, the parameter a_r is negative and physically incorrect. Finally, Region **G** cannot possess any kind of critical points, where mathematically, Eq. (15) does not have real roots.

2.1. Setting up EOS Parameters

Now we know at least the proper range of parameters for the present EOS, based on the requirement for the existence of the VLE critical point. In order to set up physically realistic EOS parameters, a, b, c, d, and Z_c, other constraints are needed. Ordinary pure substance has the solid-liquid-vapor triple point, and the condition of the triple point existence can be used for that purpose.

The triple point, that is, the solid-liquid-vapor equilibrium (SLVE), is obtained by solving the following set of equations, using the Maxwell's equal-area construction between equilibrium phases α and β.

$$P_r(V_\alpha - V_\beta) = \int_{V_\beta}^{V_\alpha} P_r \, dV_r = \frac{T_r}{Z_c(b_r - c_r)} \left\{ b_r \ln \frac{V_\alpha - b_r}{V_\beta - b_r} - c_r \ln \left| \frac{V_\alpha - c_r}{V_\beta - c_r} \right| \right.$$
$$\left. + d_r \ln \frac{V_\beta - b_r}{V_\alpha - b_r} \left| \frac{V_\beta - c_r}{V_\alpha - c_r} \right| \right\} + \frac{a_r}{Z_c^2} \left(\frac{1}{V_\alpha} - \frac{1}{V_\beta} \right). \tag{16}$$

The subscripts, α and β, represent solid and liquid (SLE), solid and vapor (SVE), and vapor and liquid (VLE).

With this additional information of the triple-point existence (triple-point temperature and pressure, T_{rt} and P_{rt}), the necessary EOS parameters can be obtained. To do so, we use the following strategy:

(1) Select proper values in b_r and Z_c from the chart in Fig. 3.

(2) Obtain a_r, c_r, and d_r using Eqs. (12) to (14): the critical point conditions.

(3) By keeping Z_c, c_r, and d_r constant, obtain new values in a_r and b_r, (a_{rt}, b_{rt}), so as to satisfy a set of Eq. (16) with desired T_{rt} and P_{rt}: the triple point condition. Here, a two-dimensional Newton–Raphson method can be employed for the numerical analysis.

(4) Check the proper order: $b_{rt} < d_r < c_r$. This is required because the EOS must be the proper topological shape even at the triple point. If it is not satisfied, go back to (1) and try another set.

(5) If temperature-independent parameters are desired, i.e., $a_{rt} = a_r$ and $b_{rt} = b_r$, then go back to (1). Repeat the process, until this condition is met.

For example, parameters thus obtained are: $a_r = a_{rt} = 0.4215$, $b_r = b_{rt} = 0.3222$, $c_r = 0.3692$, $d_r = 0.3598$, $Z_c = 0.3753$, with $T_{rt} = 0.4374$ and $P_{rt} = 0.01114$. With these constants, Eq. (6) predicts the VLE critical point, the SLV triple point, and two-phase boundaries for VLE, SLE, and SVE. Various thermodynamic properties at the triple point are calculated to be not unrealistic for typical simple substances. However, in order for the properties to be numerically more accurate, the temperature dependence of some of the parameters is required. This situation is the same as for the case of the general van der Waals EOS, Eq. (2), and it is discussed in the following section.

2.2. T-Dependence of $a(T)$ and $b(T)$ Parameters

The previous section described how to set up the EOS parameters using the VLE critical point and the triple-point condition. The parameters a_r and b_r obtained from the critical point and those from the triple point a_{rt} and b_{rt} are generally different. This means both parameters have a temperature dependence. In this section, we explore proper T-dependent functions for these parameters: $a(T)$ and $b(T)$.

Although they are empirical functions, there is some theoretical guidance to the general shape and constraint. First, both parameters are (non-zero) finite for all temperatures, including T at 0 and ∞ K. Secondly, $a(T)$

has a maximum, as shown below. The third law of thermodynamics (Nernst's theorem) states entropy, S, tends to zero at 0 K. Then, using the Maxwell relation, $(\frac{\partial P}{\partial T})_V = (\frac{\partial S}{\partial V})_T$, the following condition results:

$$\left(\frac{\partial P}{\partial T}\right)_V = 0 \qquad \text{for} \quad T = 0. \tag{17}$$

Applying this condition to the present EOS, Eq. (5), we arrive at:

$$\frac{da}{dT} = \frac{RV_0^2}{V_0 - b}\left(\frac{V_0 - d}{V_0 - c}\right), \tag{18}$$

where V_0 is a molar volume of solid (crystal) at 0 K, and a relation, $b < V_0 < d < c$, always holds in the solid-phase branch of the present EOS. This means $da/dT > 0$ (positive slope) at $T = 0$ K, since the right-hand side of Eq. (18) is positive. On the other hand, in high-temperature regions, $a(T)$ is known to be a decreasing function, i.e., $da/dT < 0$ (negative slope), as exemplified in the empirical Redlich–Kwong EOS [5], where $a(T) = 1/\sqrt{T}$. It should be also mentioned that the nature of the negative slope in $a(T)$ can theoretically be proved by calculating the second virial coefficient, $B(T)$, under a high temperature approximation while assuming a physically reasonable intermolecular potential such as the Lennard-Jones potential. Therefore, at a very low temperature, $a(T)$ must possess a maximum.

Thus, we propose the following form for $a(T)$ as one of the proper functions, which satisfy the above arguments.

$$a_r(T_r) = a_0 + a_1 T_r \exp(-a_2 T_r^n) \tag{19}$$

where a_0, a_1, a_2, and n are all positive. $a_r(0 \text{ or } \infty) = a_0$, $da_r/dT_r = a_1$ at $T_r = 0$ K, and the maximum occurs at $T_r = (na_2)^{-1/n}$.

Concerning $b(T)$, the choice is made solely based on a finitely-bounded and positive function for all temperatures:

$$b_r(T_r) = b_0 + b_1 \exp(-b_2 T_r^m), \tag{20}$$

where $b_0 > 0$, $b_2 > 0$, $m > 0$, and $b_r(0) = b_0 + b_1 > 0$. However, an important constraint among these parameters is that a relation, $b_r(T_r) < d_r$, must be satisfied for all temperatures, in order for the EOS to be the proper topological shape as discussed in the earlier sections.

The method to determine the adjustable constants in Eqs. (19) and (20) is described in a later section, when applied to real substances.

2.3. Thermodynamic Derived Functions

Although the derivation is straightforward for the present EOS form, Eq. (6), or Eq. (10), some thermodynamic property functions for pure compounds may be useful and convenient for the application, with their explicit forms. Here, we assume a_r and b_r parameters to be temperature dependent.

The fugacity coefficient ϕ is given by:

$$\ln \phi = Z - 1 - \ln Z - \int_\infty^{V_r} (Z-1)/V_r \, dV_r = Z - 1 - \ln Z - I_1,$$

where

$$I_1 \equiv \frac{1}{c_r - b_r} \left\{ c_r \ln \left| 1 - \frac{c_r}{V_r} \right| + d_r \ln \left| \frac{V_r - b_r}{V_r - c_r} \right| - b_r \ln \left| 1 - \frac{b_r}{V_r} \right| \right\} + \frac{a_r}{T_r V_r Z_c}. \tag{21}$$

The residual property, $\Delta M'$, is defined here as $\Delta M' \equiv M$ (real state) $-$ M (ideal-gas state). Then, for the reduced residual entropy, it leads to:

$$\Delta S'/R = T_r \int_\infty^{V_r} \left(\frac{\partial Z}{\partial T_r} \right)_{V_r} \bigg/ V_r \, dV + \int_\infty^{V_r} (Z-1)/V_r \, dV_r + \ln Z = I_1 + I_2 + \ln Z,$$

where

$$I_2 \equiv \left(\frac{db_r}{dT_r} \right) \frac{d_r - c_r}{(c_r - b_r)^2} \ln \left| \frac{V_r - b_r}{V_r - c_r} \right| + \frac{b_r - d_r}{V_r - b_r} + \left(\frac{da_r}{dT_r} - \frac{a_r}{T_r} \right) \frac{1}{V_r Z_c}. \tag{22}$$

For the reduced residual enthalpy, it is expressed as

$$\Delta H'/RT_c = T_r^2 \int_\infty^{V_r} \left(\frac{\partial Z}{\partial T_r} \right)_{V_r} \bigg/ V_r \, dV_r + T_r(Z-1) = T_r I_2 + T_r(Z-1). \tag{23}$$

The reduced isochoric heat capacity is:

$$\begin{aligned}
\Delta C_v'/R = T_r \int_\infty^{V_r} \left(\frac{\partial^2 P_r}{\partial T_r^2} \right)_{V_r} dV_r &= \frac{1}{V_r - b_r} \left\{ \frac{D_2(c_r - d_r)}{(c_r - b_r)^2} + \frac{D_1(b_r - d_r)}{c_r - d_r} \right\} \\
&+ \frac{D_2(c_r - d_r)}{2(V_r - b)_r^2 (b_r - c_r)} - \frac{b_r - d_r}{(b_r - c_r)^2} \left(\frac{D_2}{b_r - c_r} + D_1 \right) \ln \left| \frac{V_r - c_r}{V_r - b_r} \right| \\
&+ \frac{T_r}{V_r Z_c} \left(\frac{d^2 a_r}{dT_r^2} \right),
\end{aligned} \tag{24}$$

where

$$D_1 \equiv T_r \left(\frac{db_r}{dT_r} + T_r \frac{d^2 b_r}{dT_r^2} \right), \qquad D_2 \equiv 2T_r^2 \left(\frac{db_r}{dT_r} \right)^2.$$

The second virial coefficient is in the reduced form:

$$B(T_r)/V_c = b_r(T_r) + c_r - d_r - \frac{a_r(T_r)}{T_r Z_c}. \tag{25}$$

The other properties, coefficient of thermal expansion, $\alpha_P = (1/V)(\partial V/\partial T)_P$, isothermal bulk compressibility, $\beta_T = (-1/V)(\partial V/\partial P)_T$, isobaric heat capacity (C_p), speed of sound (u), etc. are similarly derived in analytically closed forms: $C_p = C_V + TV\alpha_P^2/\beta_T$, $u^2 = (C_p/C_V)(V/M\beta_T)$, where M is the molar mass.

3. APPLICATIONS

In this section, we first apply the proposed EOS to actual pure substances: Ar (argon), CO_2 (carbon dioxide), and CH_4 (methane). Ar is often a standard compound to check the validity of EOS. If it is well presented by any theoretical model, all other classical monoatomic compounds such as Ne, Xe, and Kr, except for the quantum fluid (He), should also be modeled properly with the same model, since the principle of corresponding states works well among these noble gases. Similarly, it is expected to work well for nonpolar and spherical molecules like CH_4. Among so-called "simple" fluids, CO_2 has some unique thermodynamic properties. The triple-point (reduced) temperature of about 0.7 is the highest, and thus the "normal boiling" point, i.e., at one atmosphere, does not exist; it becomes the "normal sublimation" point, being in the solid/vapor equilibrium state [21]. Although it is classified as a nonpolar compound by the general definition without having a permanent electric dipole moment, its molecular quadrupole moment is large, and it behaves like a polar compound in some of the thermodynamic properties [22]. The molecular shape is not spherical, being different from Ar and CH_4. Thus, the applicability to CO_2 may provide a further validity test for the present EOS.

Next, we examine whether the present EOS can be applied to mixture phase properties, using a binary system of CO_2/CH_4. This system is not only important for industrial applications, but also challenging, since the phase behavior is far from being an ideal mixture. In addition, the triple-point locus of the solid-liquid-vapor equilibrium shows a peculiar shape,

due to the interaction of the solid phase of CO_2 and the supercritical fluid of CH_4 in certain temperature/pressure conditions [23, 24].

The third example is an application to hard-sphere ensembles. Although the hard sphere is purely a model "compound," many studies and significant contributions have been made in the theory of statistical physics and thermodynamics [9].

3.1. Pure Compounds: Ar, CO_2, and CH_4

How accurately the thermodynamic behaviors and properties of real substances are modeled by a proposed EOS depends upon the type of EOS, the number of adjustable EOS parameters, and how many and what kind of experimental data are used to determine the adjustable parameters. The present purpose is to demonstrate the feasibility of the proposed EOS for actual substances, not the presentation with a numerically high accuracy. Thus, we use a minimum amount of information to set up the EOS parameters: the conditions of VLE critical point and the triple point. The basic strategy to set up the proper EOS parameters in this way has been described in Sections 2.1 and 2.2, although it is neither unique nor the best. Here we follow this methodology.

The proper EOS parameters can be obtained, using the strategy (1) through (4) in Section 2.1, together with a further constraint about the liquid volume information of the triple point: not necessarily being exact, but at least being reasonably close. This process can be rather easily made. Then, we have the two sets of a_r and b_r parameters: (a_{rc}, b_{rc}) at $T_r = 1$, and (a_{rt}, b_{rt}) at $T_r = T_{rt}$. Next, we have to find out the T-dependence of these parameters in Eqs. (19) and (20). These equations contain four adjustable parameters within themselves, with certain restrictions as discussed in Section 2.2. At least two parameters in each equation can be determined from these two sets of a_r and b_r parameters. For further constraints to fix those parameters, the information about the Boyle-point temperature, T_{rB}, and the maximum inversion temperature of Joule–Thomson's coefficients, T_{rJT} can be used. The Boyle point, where the second virial coefficient becomes zero, is determined from Eq. (25). T_{rJT} is determined from the relation: $B/T_{rJT} = (dB/dT_r)$, where B is given by Eq. (25). For noble gases, T_{rB} is about 2.7 and T_{rJT} is about 5.1 [4]; for CO_2 and CH_4, T_{rB} is 2.37 and 2.67, respectively [21, 26].

To make the analysis a little easier, we assumed rather arbitrarily $b_2 = (1/0.75)^m$ in Eq. (20). Then, adjusting the exponent m and n in Eq. (19) by some trials and errors, we obtained all necessary parameters in Eqs. (19) and (20) so as to satisfy the restrictions and constraints mentioned above. Although they are not necessarily unique, nor optimal, the

Table I. EOS Constants in Eq. (6)

	c_r	d_r	Z_c
Ar	0.34598	0.33717	0.37510
CH_4	0.33739	0.33020	0.37503
CO_2	0.34017	0.32309	0.37510

Table II. EOS Constants for a_r and b_r in Eq. (6), Using Eqs. (19) and (20)

	a_0	a_1	a_2	n	b_0	$b_1 (\times 10^{-2})$	b_2	m
Ar	0.35440	52.5178	6.65460	0.404	0.32400	-2.25797	17.7577	10
CH_4	0.32027	147.615	7.30936	0.309	0.32608	-2.32890	5.61866	6
CO_2	0.28578	82.0637	6.40361	0.424	0.31588	-4.90960	5.61866	6

Table III. Thermodynamic Properties of Argon at the Triple Point[a]

	$\Delta V_{ls}/V_s$ (%)	$\Delta S_{ls}/R$	$\Delta S_{lv}/R$	C_v/R	C_P/R	u (m·s^{-1})	$\ln Z$	$\beta_T (\times 10^{-3})$ (MPa^{-1})	$\alpha_P (\times 10^{-3})$ (K^{-1})
Calc.	15.6	1.72	9.85	3.56	5.99	908	-5.63	1.44	3.08
Obs.	15.0	1.69	9.39	2.64	5.36	863	-5.88	1.93	4.29

[a] Property comparison between the present model calculation (Calc.) and observed (Obs.) values [16, 33]. $\Delta V_{ls}/V_s$: relative volume change from solid to liquid. $\Delta S_{ls}/R$: entropy change from solid to liquid. $\Delta S_{lv}/R$: entropy change from liquid to vapor. C_v/R: isochoric heat capacity of liquid. C_P/R: isobaric heat capacity of liquid. u: speed of sound of liquid. Z: compressibility factor of liquid. Isothermal bulk compressibility of liquid, $\beta_T = (-1/V)(\partial V/\partial P)_T$. Coefficient of liquid thermal expansion, $\alpha_P = (1/V)(\partial V/\partial T)_P$.

Table IV. Thermodynamic Properties of Methane at the Triple Point[a]

	$\Delta V_{ls}/V_s$ (%)	$\Delta S_{ls}/R$	$\Delta S_{lv}/R$	C_v/R	C_P/R	u (m·s^{-1})	$\ln Z$	$\beta_T (\times 10^{-3})$ (MPa^{-1})	$\alpha_P (\times 10^{-3})$ (K^{-1})
Calc.	12.0	1.76	12.2	4.35	6.59	1883	-7.23	0.95	2.04
Obs.	–	1.24	8.84	4.18	6.50	1539	-7.50	1.45	2.95

[a] See the footnote of Table III for the meaning of symbols. Obs. [26].

Table V. Thermodynamic Properties of Carbon Dioxide at the Triple Point[a]

	$\Delta V_{ls}/V_s$ (%)	$\Delta S_{ls}/R$	$\Delta S_{lv}/R$	C_v/R	C_P/R	u (m·s^{-1})	$\ln Z$	β_T ($\times 10^{-3}$) (MPa^{-1})	α_P ($\times 10^{-3}$) (K^{-1})
Calc.	27.7	4.97	10.0	4.43	13.0	1186	−4.22	1.78	3.39
Obs.	28.4	4.79	8.56	5.16	10.3	976	−4.53	1.79	3.08

[a] See the footnote of Table III for the meaning of symbols. Obs. [21].

sets of parameters obtained for Ar, CH_4, and CO_2 are listed in Tables I and II.

Now that the EOS parameters have been set up, we can predict various thermodynamic properties and phase behaviors for these compounds. Some calculated properties at the triple point are shown in Tables III, IV, and V, compared with available experimental data for Ar, CH_4, and CO_2. The global phase diagrams of Ar and CO_2 are given in Figs. 4 to 7, compared with some selected observed data. Although they are not shown here, similar results have been obtained for CH_4. These comparisons show that the present EOS can describe the solid, liquid, and vapor phases reasonably well for these simple compounds.
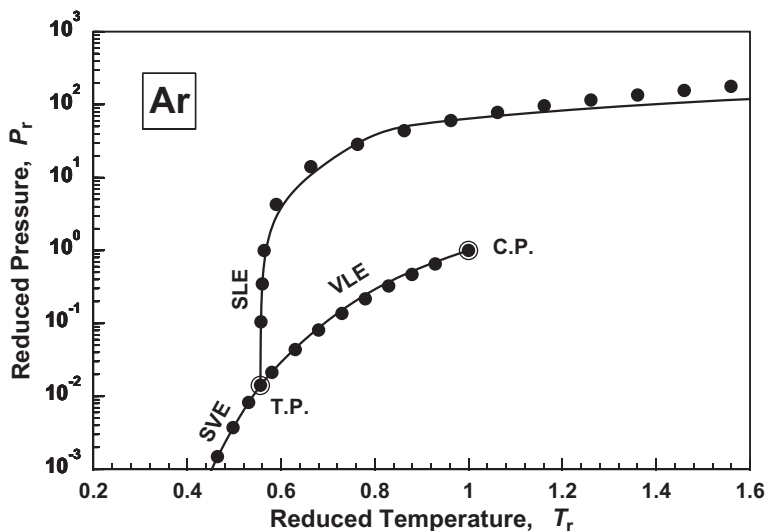
Fig. 4. Phase diagram of argon in the *TP* projection. Lines: calculated with the present EOS. Symbols: selected experimental data [33].
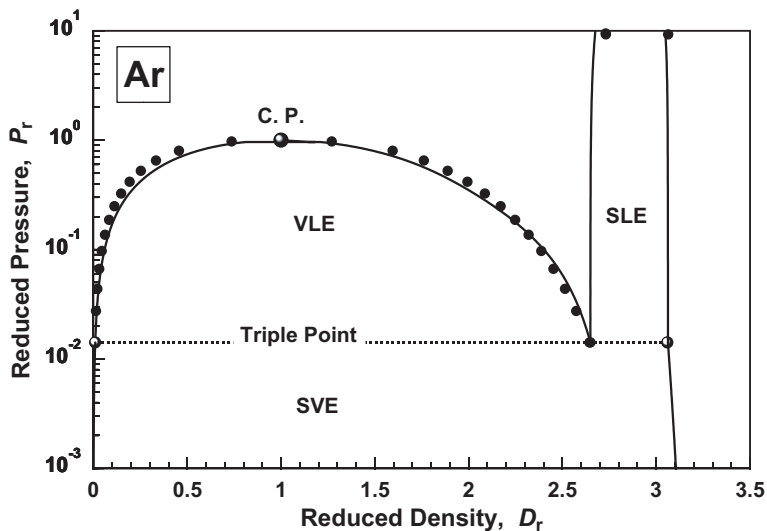
Fig. 5. Phase diagram of argon in the pressure-density projection. Lines: calculated with the present EOS. Symbols: selected experimental data [33].
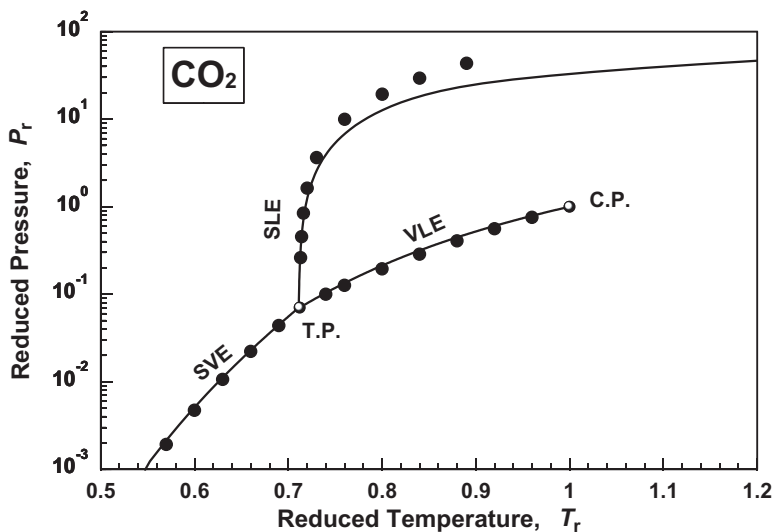
Fig. 6. Phase diagram of carbon dioxide in the TP projection. Lines: calculated with the present EOS. Symbols: selected experimental data [21].
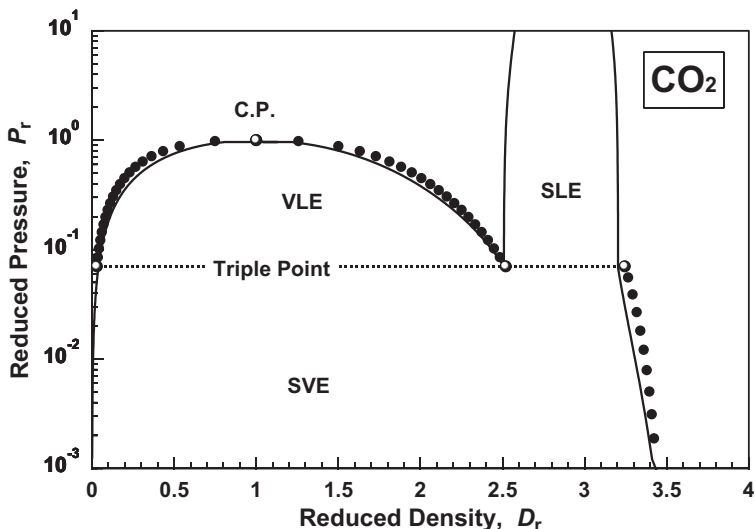
Fig. 7. Phase diagram of carbon dioxide in the pressure-density projection. Lines: calculated with the present EOS. Symbols: selected experimental data [21].

3.2. Mixtures: CO_2/CH_4

An interesting challenge is to see whether the present EOS can be applied to the mixture's phase behavior as well, particularly for the case involved in the solid phase. To do so, we employ the conventional mixing rule with the pure component EOS parameters, and also the non-reduced EOS form in Eq. (5), in order to avoid the unknown reducing (critical) parameters for mixtures.

$$Z = \frac{PV}{RT} = \frac{V(V-d)}{(V-b)(V-c)} - \frac{a}{VRT} \qquad (26)$$

Here, the mixing and combining rules for a, b, c, and d parameters are modeled by the so-called van der Waals/Lorentz–Berthelot rules with k_{ij},

$$a = \sum_{i,j=1}^{N} \sqrt{a_i a_j}(1-k_{ij})\, x_i x_j \qquad (27)$$

$$b = \sum_{i=1}^{N} b_i x_i, \qquad c = \sum_{i=1}^{N} c_i x_i, \qquad d = \sum_{i=1}^{N} d_i x_i, \qquad (28)$$

where k_{ij} is an adjustable parameter, which is often called the binary interaction parameter: $k_{ii} = 0$, and $k_{ij} = k_{ji}$. The fugacity coefficient for the ith species in N component mixtures is calculated by the following standard thermodynamic equation [2]:

$$\ln \phi_i = \int_V^\infty \left[\left(\frac{\partial n Z}{\partial n_i} \right)_{T, nV, n_j} - 1 \right] \frac{dV}{V} - \ln Z. \tag{29}$$

Then, for the present EOS it leads to:

$$\ln \phi_i = \frac{1}{b-c} \left[c \ln \left| 1 - \frac{c}{V} \right| - b \ln \left(1 - \frac{b}{V} \right) \right]$$

$$- \frac{c_i(b-d) + b_i(d-c) + (b-c)(d-d_i)}{(b-c)^2} \ln \left| \frac{V-c}{V-b} \right|$$

$$- \frac{1}{b-c} \left[\frac{c_i(c-d)}{V-c} + \frac{b_i(d-b)}{V-b} \right] - \frac{2 \sum_{j=1}^N \sqrt{a_i a_j}(1-k_{ij}) x_j}{V RT} - \ln Z. \tag{30}$$

Similarly, other thermodynamic properties of mixtures, such as enthalpy, entropy, heat capacity, etc. can be written in analytically closed forms.

An example taken here is a binary system of CO_2/methane mixtures, in which methane VLE and supercritical phases are intercepted by the CO_2 solid phase, and a three-phase (SLVE triple point) locus arises [23, 24]. The three-phase equilibrium is solved by the usual thermodynamic equilibrium conditions:

$$\phi_i^S x_i^S = \phi_i^L x_i^L = \phi_i^V x_i^V, \qquad i = 1, 2 \quad (1 \text{ for methane, and 2 for } CO_2) \tag{31}$$

where superscripts, S, L, and V represent the solid, liquid, and vapor phases, respectively, and each phase has the same temperature and pressure. The three-phase equilibrium in a binary system is a univariant state according to the Gibbs phase rule, and thus with a given temperature, the corresponding pressure and each phase composition (mole fraction, x_i) can be completely determined by solving the above equations.

In order to obtain the numerical solution of these equations, the binary interaction parameter, k_{ij}, must be set properly. k_{ij} is expected to be about 0.09 to 0.15 for this binary system, since it is known in the fluid state [27] to be 0.0973 for CO_2/methane [for Soave–Redlich–Kwong EOS] and 0.15 for CO_2/hydrocarbons [for Peng–Robinson EOS]. It has been found from trials and errors that k_{ij} of about 0.10 to 0.12 is a proper value

for the present EOS. The calculated results for SLVE phase behaviors with $k_{ij} = 0.117$ are shown in Figs. 8–10. With the same k_{ij}, a VLE Px diagram has been also calculated at 230 K and compared with the experimental values [28] in Fig. 11.

It may be fair to say that the present model predictions are in good agreement with the observed data, using only one adjustable parameter, k_{ij}. Tillner-Roth also modeled successfully this challenging system using highly accurate fluid EOS for both pure compounds, combined with a separate and different thermodynamic equation for the solid CO_2, where the solid state of mixtures was assumed to be pure CO_2 [12]. The present model prediction for the SLVE triple-point locus seems in better agreement with the experimental data [23, 24]. The solid phase is predicted in our model to be a mixture containing a small amount of methane.

3.3. Hard-Sphere Phase Transition

The hard-sphere model has played significant roles on various important developments in statistical physics and thermodynamics [9]. One of the remarkable things is that the equation of state for hard-sphere ensembles has been solved analytically [26], based on the Percus–Yevick approximation of the exact integral equation for the radial distribution (or direct correlation) function in the theory of liquids. However, the derived EOS did not show any phase transition (or singularity) within the physically meaningful region. On the other hand, other approximations, the Kirkwood equation or the Yvon–Born–Green equation, cannot be solved analytically, but by numerical analyses Kirkwood and Boggs [30] predicted an instability of the fluid state, well below the closest packing density of the solid, indicating the possible fluid/solid phase transition for hard spheres. Later, Alder and Wainwright [14] and Wood and Jacobson [31] confirmed such a phase transition by computer simulations ("experiments") using molecular dynamics for the former and the Monte Carlo method for the latter. This fascinating phenomenon of hard spheres is sometimes called the "Alder Transition."

By use of the computer "experiments" while imposing the thermodynamic equilibrium condition, Hoover and Ree [32] obtained the transition densities, ρ_S (solid), ρ_L (liquid), and compressibility factor, Z_{SL}:

$$\rho_S / \rho_0 = 0.736 \pm 0.003$$
$$\rho_L / \rho_0 = 0.667 \pm 0.003$$
$$Z_{SL} = P / \rho_0 kT = 8.27 \pm 0.13$$
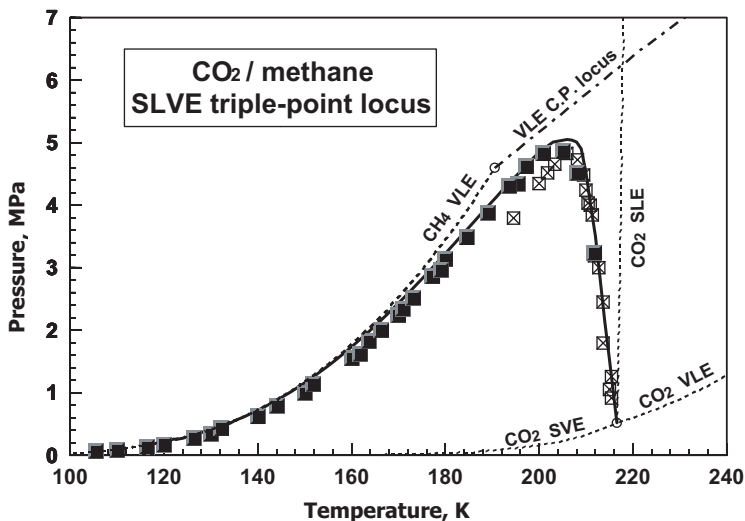
Fig. 8. Solid-liquid-vapor triple point locus of binary mixtures of CO_2 and CH_4. The two-phase lines and critical-point locus are also shown. Lines: calculated with the present EOS model. Symbols: experimental data, solid symbols [24] and open symbols [23].
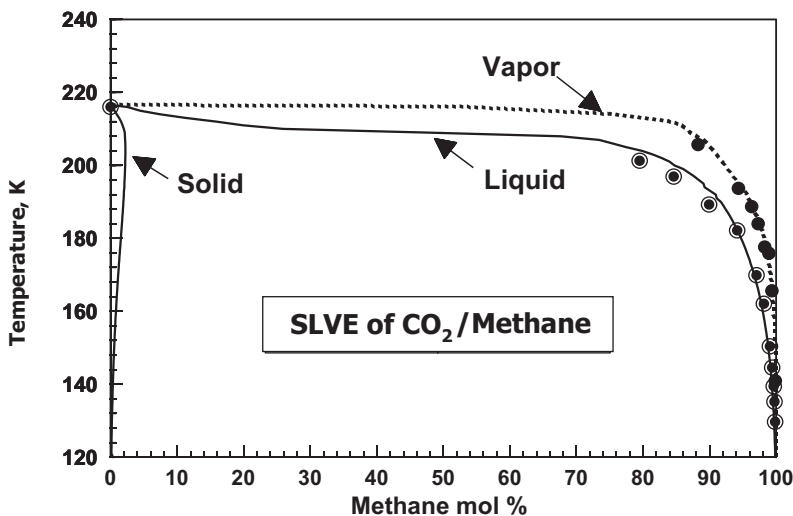
Fig. 9. Temperature-composition diagram of the solid-liquid-vapor triple point locus of binary mixtures of CO_2 and CH_4, shown in Fig. 8. Lines: calculated with the present EOS model. Symbols: experimental data [24].
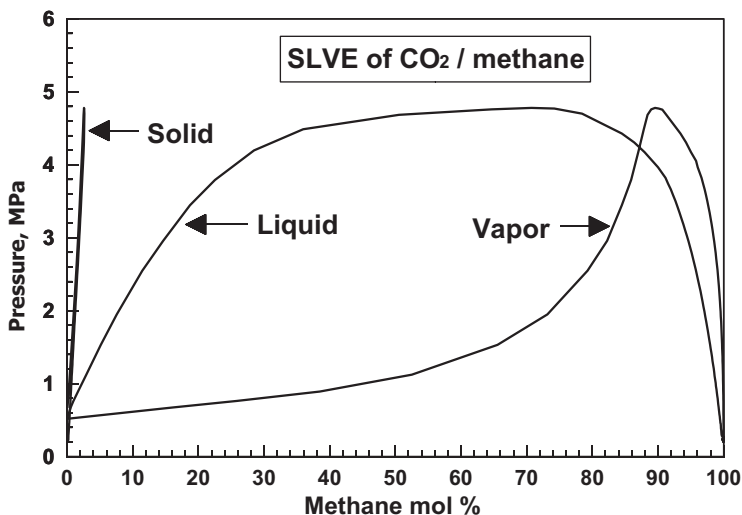
Fig. 10. Pressure-composition diagram of the solid-liquid-vapor triple point locus of binary mixtures of CO_2 and CH_4, shown in Fig. 8. Lines: calculated with the present EOS model.
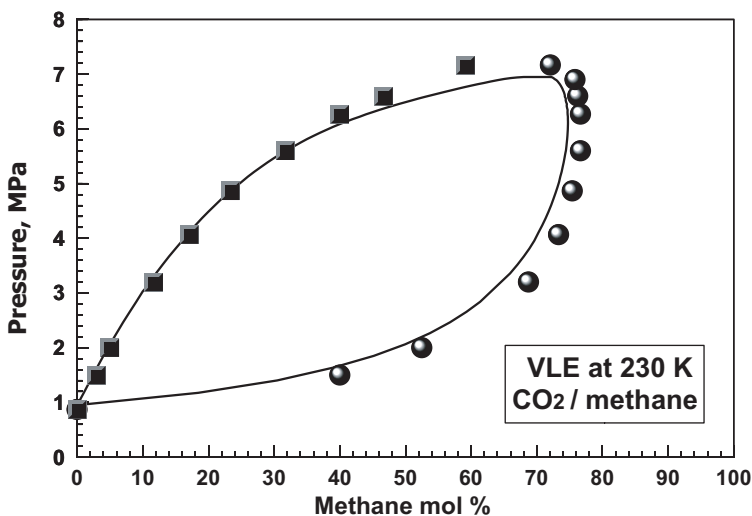
Fig. 11. Isothermal pressure-composition diagram of vapor-liquid equilibria for binary mixtures of CO_2 and CH_4 at $T = 230$ K. Lines: calculated with the present EOS. Symbols: experimental data [28].

where ρ_0 is the closest packing density of hard spheres (diameter of σ): $\rho_0 = \sqrt{2}/\sigma^3$.

It is interesting to see whether the present simple EOS can predict similar results. In our case, the hard-sphere EOS becomes, by setting $a = 0$ in Eq. (5) and being reduced with $V_0 = N_A/\rho_0$, [N_A is the Avogadro's number]:

$$Z_{SL} = \frac{PV_0}{RT} = \frac{V_h - d_h}{(V_h - b_h)(V_h - c_h)} \tag{32}$$

where $V_h \equiv V/V_0$, $b_h \equiv b/V_0$, $c_h \equiv c/V_0$, and $d_h \equiv d/V_0$. Then, the phase-equilibrium condition, i.e., the Maxwell's equal-area construction, is given by:

$$\begin{aligned}
Z_{SL}(V_{hL} - V_{hS}) &= \int_{V_{hS}}^{V_{hL}} \frac{V_h - d_h}{(V_h - b_h)(V_h - c_h)} \, dV_h \\
&= \frac{1}{b_h - c_h} \left\{ (b_h - d_h) \ln \left| \frac{V_{hL} - b_h}{V_{hS} - b_h} \right| + (d_h - c_h) \ln \left| \frac{V_{hL} - c_h}{V_{hS} - c_h} \right| \right\}.
\end{aligned} \tag{33}$$

Since $V_{hS}(= \rho_0/\rho_S)$ and $V_{hL}(= \rho_0/\rho_L)$ are roots of the quadratic equation Eq. (32) and can be analytically solved, the coupled nonlinear equations, Eqs. (32) and (33), are easily solved for V_{hS}, V_{hL}, and Z_{SL} by the ordinary Newton–Raphson method, with a specified set of (b_h, c_h, d_h) parameters. Or, vice versa, a set of parameters, b_h, c_h, d_h, can be similarly obtained with given values in $V_{hS}(= \rho_0/\rho_S)$, $V_{hL}(= \rho_0/\rho_L)$, and Z_{SL}.

Here we use the parameter (b_r, c_r, d_r) set obtained in the analysis of Ar at $T \to \infty$ [see Section 3.1]. Then, the following phase-transition parameters result, with a normalization factor of $V_c/V_0 = 4.082$:

$$\rho_S/\rho_0 = 0.735$$
$$\rho_L/\rho_0 = 0.668$$
$$Z_{SL} = P/\rho_0 kT = 8.14.$$

These are in excellent agreement with those by Hoover and Ree [32] mentioned above. Furthermore, from the normalization factor of 4.082 and the observed argon V_c of 74.59 cm$^3 \cdot$ mol^{-1} [30], the hard-sphere diameter, σ, for Ar is calculated to be 0.350 nm. It is quite reasonable, compared with the literature values: 0.340 to 0.347 [25] and 0.354 nm [34]. This means the hard-sphere model very well describes the solid/liquid transition of Ar, as demonstrated by Longuet-Higgins and Widom [13], using the computer "experimental" data.

It should be mentioned briefly here about the virial coefficients of hard spheres, since many efforts in the past have been made to calculate the virial equation of state. Among the infinite number of coefficients, only the first seven or eight coefficients have been calculated by the exact integration method [35, 36]. The profound complexity of the cluster integrals inhibits further calculations. A challenge to extending more coefficients is still an active research area [36–38]. So far, there is no indication of the solid-fluid phase transition [38]. However, one must bear in mind that the virial equation of state is valid only for the fluid (low and medium density) state. In fact, it is in excellent agreement with the fluid branch of the computer "experiment" of hard spheres. The hard-sphere virial coefficients by the present EOS will be discussed in a later section.

4. DISCUSSIONS

Computer "experiments" with the Monte Carlo or molecular dynamics method provide useful information including the solid state for model compounds, such as Lennard-Jones fluids and hard spheres. With ever-improving computer power, this type of work will bring us further valuable insights of various phase behaviors of complicated systems. A recent review paper [39] describes such research activities.

With regard to a useful statistical model describing solid (gas hydrate) systems, the van der Waals–Platteeuw theory is well known [40], and successful applications to real substances have been demonstrated [41]. Recently, an attempt to formulate a unified solid-liquid-vapor EOS model has been reported based on the cell theory [42]. However, the EOS is not analytically closed, and the predicted results are quite disappointing: predicting a negative triple-point pressure, negative pressures in VLE, and even worse the disappearance (critical point) of the solid-liquid phase transition which is qualitatively incorrect.

The present approach to understand the solid-liquid-vapor states of matter in a single unified EOS is empirical, but the proposed EOS satisfies the known thermodynamic observations. Also it is simple, analytical, and able to be applied to actual cases with reasonable accuracy. In the following subsections, we will discuss the present EOS, concerning further improvements, limitations, possible applications, and related matters.

4.1. Pure Compounds

The proposed empirical EOS would be the simplest analytical form to describe the solid-liquid-vapor state in a unified way, and can be regarded as a physically reasonable extension of the original van der Waals fluid

EOS. By allowing the proper temperature dependence on some of the EOS parameters, thermodynamic properties of simple substances such as noble gases, methane, and carbon dioxide have been modeled with reasonable accuracy, including the solid phase. The present demonstration is rather to show the feasibility of this new EOS, using limited experimental information: the VLE critical point and the triple point. It is certainly possible to model the property of real compounds more accurately, by fitting more experimental data such as the vapor pressure curve, saturated liquid densities, heat capacity data, and so forth. In addition to the temperature dependence on the a and b parameters in Eq. (5), the c and/or d parameters may be treated as being T-dependent as well, in order to improve the accuracy in the actual application, although the thermodynamically derived functions and analyses will become more complicated.

Another improvement in the accuracy will be the use of the more general form of Eq. (4). In the present simplest case, the critical compressibility factor Z_c is larger than 0.375, essentially the same as that of the original van der Waals EOS. This is due to the use of the original van der Waals attraction form, and limits the numerical accuracy in vapor density since Z_c is close to 0.3 for many actual compounds. This situation can be improved by the use of $q = 1$ and $r = 0$, or $q = 2$ and $r = -1$ in Eq. (4), as well known in the general cubic EOS [Eq. (2)]. The use of k value larger than one in Eq. (4) may also improve the numerical accuracy, particularly in condensed phase properties, based on the discussion in Section 4.2.

It should be emphasized here that the present EOS is only valid for so-called "simple" fluids, which does not necessarily mean compounds with small molecular sizes. For example, water is regarded as a "complex" compound with the hydrogen bonding. The solid state ice has several modifications, and does not form the closest-packing structures, where the solid density is smaller than the liquid and the melting curve shows the negative slope for the Ice-I modification [43]. In general, solids have multiple modifications with different crystal symmetries. The present EOS does not consider such different symmetries of the solid state.

4.2. Hard Spheres

As mentioned in Section 3.3, it may be worthwhile to discuss the virial coefficient of the hard-sphere system, although it is only for the fluid-only state. The hard-sphere model [Eq. (32)] of the present EOS applies for both fluid and solid phases, where the virial expansion turned out to be nearly the same as the repulsive core P_{HC} of van der Waals. The purpose of the present work is not to develop an accurate equation for the fluid branch. For that purpose the excellent empirical equation has already been

developed by Carnahan and Starling [8]. However, it is interesting to simulate the fluid-phase virial coefficients, by making Eq. (32) have only a fluid branch: i.e., by assigning appropriate values in the EOS constants (b, c, and d), or in other words by removing the present EOS parameter restrictions [see Section 2]. For this purpose, we use the more general P_{HC} form in Eq. (4), instead of Eq. (32):

$$Z = \frac{V}{V-b} \left(\frac{V-d}{V-c} \right)^k = \left(1 - \frac{b}{V} \right)^{-1} \left(1 - \frac{d}{V} \right)^k \left(1 - \frac{c}{V} \right)^{-k}. \quad (34)$$

This can be analytically expanded and rearranged as the following virial expansion form with the dimensionless coefficient B_i:

$$Z = 1 + \sum_{i=2}^{\infty} B_i \left(\frac{2\pi\sigma^3}{3} \right)^{i-1} \left(\frac{1}{V} \right)^{i-1}, \quad (35)$$

where B_i is a function of b, c, and d, which are assumed here to be dimensionless, being normalized by a volume, $2\pi\sigma^3/3$.

With a given k value, we have three adjustable parameters (b, c, and d), which can be determined so as to reproduce the well-known three (exact) values ($B_2 = 1$, $B_3 = 0.625$, and $B_4 = 0.2869$) [9, 35, 36]. Then we look at the behavior of the other coefficients that give us some idea about the accuracy of the present EOS *form* for the repulsive part P_{HC}. Five cases with $k = 1$, 2, 3, 4, and 5 have been calculated up to B_8. The results are compared in Table VI with the exact virial calculations and some other models. It should be mentioned that in the case of $k = 1$, only two values (B_2 and B_3) are used assuming $b = c$, since it turned out that three real roots for b, c, and d cannot exist in this case, for the exact values, B_2, B_3, and B_4.

The increase in k values improves the higher-order virial coefficients and approaches those of the exact theoretical calculation and the Carnahan–Starling empirical equation. Although this is only for the fluid-phase branch, it suggests that the use of $k = 4$ or 5 for the present proposed EOS may improve the accuracy of solid/liquid properties. However, it must be mentioned here that the comparison of virial expansions can hardly be justified for the validity of theoretical models in the high-density region [44].

4.3. EOS Parameter Regions B and C in Fig. 3

In Section 2, we have discussed the physically proper parameters for the present EOS and summarized the results in Fig. 3. The parameters in

Table VI. Comparison of Hard-Sphere Virial Coefficients for the Fluid Phase[a]

	B_2	B_3	B_4	B_5	B_6	B_7	B_8
Exact	1	0.625	0.2869	0.1103	0.0386	0.0131	0.0040
CS	1	0.625	0.2823	0.1094	0.0391	0.0132	0.0043
PYP	1	0.625	0.2500	0.0859	0.0273	0.0083	0.0024
PYC	1	0.625	0.2969	0.1211	0.0449	0.0156	0.0052
$k=1$	1	0.625	0.3343	0.1652	0.0779	0.0355	0.0117
$k=2$	1	0.625	0.2869	0.1460	0.0524	0.0294	0.0068
$k=3$	1	0.625	0.2869	0.1295	0.0494	0.0211	0.0051
$k=4$	1	0.625	0.2869	0.1148	0.0400	0.0133	0.0040
$k=5$	1	0.625	0.2869	0.1127	0.0385	0.0122	0.0036

[a] "Exact" is the result from the exact cluster integration [36], "CS" is the Carnahan–Starling empirical equation [8], "PYP and PYC" are the Percus–Yevick analytical equations of hard spheres for the pressure and compressibility equations [9], respectively, and "$k = 1, 2, 3, 4, 5$" are the present hard-sphere model of Eq. (34).

Region **A** of Fig. 3 have been said to be physically correct for EOS behaviors and used in the present analyses. However, two other areas (Regions **B** and **C**) in Fig. 3 deserve special comments.

Region **B** provides an interesting EOS topology, where the critical point occurs inside the solid branch, and a stable fluid branch exists. An isothermal PV diagram below the critical temperature is shown in Fig. 12. This feature may be used as a local model describing peculiar behaviors observed in Cs (Cesium) and Ce (Cerium) [45, 46]. Ordinary solids do not have the solid-solid critical point, due to the different symmetry of crystal structures. At low temperatures, however, solid Ce has two modifications (α-Ce and γ-Ce) which possess the same fcc (face-centered-cubic) structures with different lattice constants, and then in the solid-solid equilibrium the critical point exists. Also, in the case of Cs, both Cs II and Cs III solids have the same fcc structure but with a smaller lattice constant for the latter. Their coexistence (iso-structural phase transition) curve ends at the solid-solid-liquid triple point around 4.25 MPa and 88°C [45].

The EOS topology in Region **C** of Fig. 3 is illustrated in Fig. 13. Here, only solid and vapor branches stably exist. This situation occurs when the parameter d becomes larger than c (and b), and is physically correct for the case for temperatures below the triple point, where no liquid state exists. Also, the first-order phase transition between the solid and vapor can be calculated with the Maxwell's equal-area construction. In the present analyses, the EOS topology is based on the Region **A** type [Fig. 1] for all
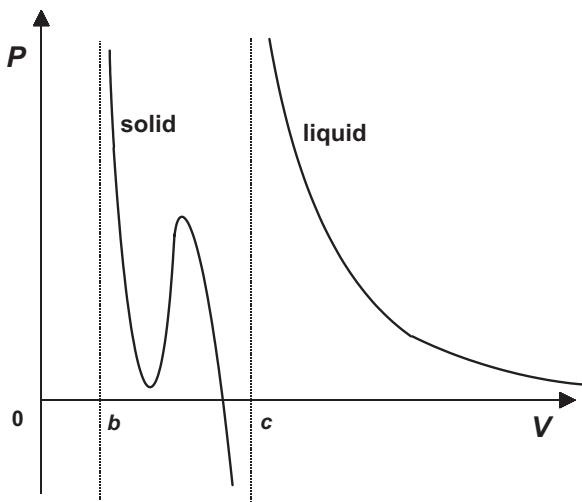
Fig. 12.   Schematic isothermal PV diagram of Eq. (5) with the EOS parameter region **B** in Fig. 3. Iso-structurual solid-solid phase transitions occur and their critical point exists at a higher temperature.
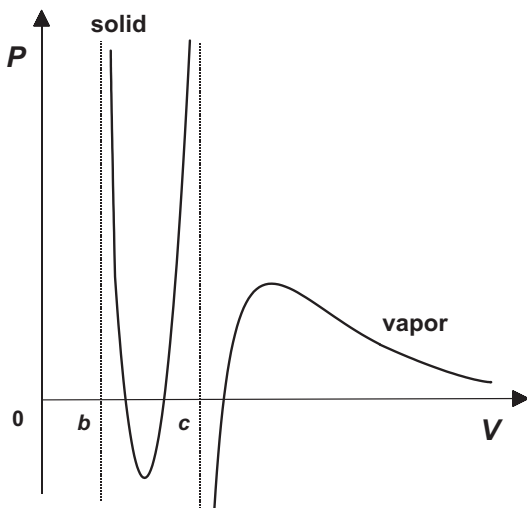
Fig. 13.   Schematic isothermal *PV* diagram of Eq. (5) with the EOS parameter region **C** in Fig. 3. No stable liquid branch exists. This topological shape represents the case of temperatures below the triple point.

temperatures. The existence of the stable liquid branch below the triple-point temperature must be regarded as supercooled liquid. This suggests the d (or c) parameter must change at *well below* the triple point in order for the EOS topology to be more physically correct. In this regard, it should be mentioned that the general EOS form, Eq. (4) with $k =$ even integer case, does not possess this type of EOS topology, and the stable liquid-phase branch always exists. Thus, an EOS with $k =$ odd integer will be more flexible and physically a better choice for modeling the entire temperature region.

4.4. Mixtures

As shown in Section 3.2, the present EOS model can be applied to mixtures as well. The example investigated there is a binary system of CO_2 (carbon dioxide) and CH_4 (methane). The observed peculiar shape of the solid-liquid-vapor triple-point locus has been successfully predicted, as shown in Fig. 8, where it shows a maximum. The Px phase diagram (Fig. 10) is more complicated than the Tx phase diagram (Fig. 9), and shows the multiplicity, reflecting the two (left and right) sides of the maximum in Fig. 8. The two sets of compositions at a given pressure in Fig. 10 may need some explanations. Each (solid, liquid, or vapor) phase has a convex shape in the pressure-composition diagram; the solid-phase "gap" is too small to be seen in the scale shown in Fig. 10. The same (left or right) side composition of each peak is the proper pair that corresponds to a set of the triple-point condition. It is quite unusual, compared with the case of the familiar three-phase locus of binary liquid-liquid-vapor triple points. Although the discussion about this particular behavior is outside the scope of the present purpose, it may be worthwhile to make some brief comments.

The curious maximum of the triple-point locus arises from the unique situation, where the supercritical fluid of CH_4 interacts with the CO_2 SVE phase. In order to obtain further insights, we use the following thermodynamic relation, which holds for the univariant (solid-liquid-vapor equilibrium) state of binary mixtures:

$$T \frac{dP}{dT} = \frac{(H^L - H^S) + r(H^V - H^S)}{(V^L - V^S) + r(V^V - V^S)} \equiv \frac{\Delta H^{L\text{-}S} + r\,\Delta H^{V\text{-}S}}{\Delta V^{L\text{-}S} + r\,\Delta V^{V\text{-}S}} \equiv \frac{\Delta H}{\Delta V}, \tag{36}$$

where $r = -\frac{x^V - x^S}{x^L - x^S} \equiv -\frac{\Delta x^{V\text{-}S}}{\Delta x^{L\text{-}S}}$, the superscripts S, L, and V refer to the solid-, liquid-, and vapor-phase property, respectively, with mole fraction x of CH_4 (or CO_2). H^α and V^α ($\alpha =$ S, L, or V) are molar enthalpy and molar volume, respectively: $H^\alpha = \sum_{i=1}^2 H_i^\alpha x_i$ and $V^\alpha = \sum_{i=1}^2 V_i^\alpha x_i$. Equation (36) can be derived without difficulty using the thermodynamic equilibrium

condition (the equality of the chemical potential among each phase), together with the Maxwell relation and the Gibbs–Duhem relation. This is an analog of the well-known Clausius–Clapeyron equation for the univariant (two-phase equilibrium) state of pure compounds, which is often used to obtain a latent heat of the first-order phase change of pure compounds.

Equation (36) is formally the same as the Clausius–Clapeyron equation, but ΔH defined here cannot be interpreted simply as the latent heat of the three-phase transition, although the triple point certainly possesses the latent heat due to the first-order phase transition. The physical meaning of ΔH in Eq. (36) is not so straightforward, but often it is interpreted as an enthalpy change of a *formal* (*decomposition or formation*) *reaction* of each phase, although no true chemical reactions are occurring [38].

Here we use Eq. (36) simply to determine a thermodynamic relation at the maximum of the triple-point locus (Fig. 8). At the maximum, $dP/dT = 0$. Then, the following relation holds at the maximum:

$$\frac{\Delta H^{L-S}}{\Delta x^{L-S}} = \frac{\Delta H^{V-S}}{\Delta x^{V-S}}. \tag{37}$$

The positive and negative (left and right side of the maximum) slope in dP/dT is due to the sign of ΔH in Eq. (36), since ΔV is always positive based on the result in Fig. 10.

As demonstrated in Section 3.2, the present EOS can quantitatively predict mixture properties including the solid phase. It is interesting to see more actual applications, including multicomponent mixtures. In addition, because of the simplicity of the present EOS form, it may become a useful tool for the topological classification of the global phase diagram of mixtures including the solid state, as remarkably done in the fluid-only case by van Konynenberg and Scott [3], using the original van der Waals EOS.

5. CONCLUSIONS

As an extension of the van der Waals fluid EOS, a simple analytical EOS for solid-liquid-vapor phases has been developed, based on fundamental thermodynamic requirements and analytical geometry. It has been demonstrated that the thermodynamic behaviors and properties of simple pure substances (argon, methane, and carbon dioxide) are modeled reasonably well with this EOS, including the well-known solid/fluid phase transition of hard spheres.

In addition, it has been shown that the present model can be applied to mixtures as well. The triple point (solid/liquid/vapor equilibrium) locus of a binary system of carbon dioxide and methane has been successfully modeled.

Although further improvements in accuracy and limitations remain to be resolved, the beauty of the present EOS is its simplicity, like the original van der Waals fluid EOS. Among others, one of the promising applications of the present simple EOS may be the classification of the global phase behavior of binary mixtures including the solid phase [17, 47].

REFERENCES

1. J. D. van der Waals, Doctoral Dissertation (Leiden, Holland, 1873).
2. J. L. Lebowitz and O. Penrose, *J. Math. Phys.* **7**:98 (1966).
3. P. H. van Konynenberg and R. L. Scott, *Philos. Trans. Roy. Soc. London Ser. A* **298**:495 (1980).
4. H. C. Van Ness and M. M. Abbott, *Classical Thermodynamics of Nonelectrolyte Solutions* (McGraw–Hill, New York, 1982).
5. O. Redlich and J. N. S. Kwong, *Chem. Rev.* **44**:239 (1949).
6. D. Y. Peng and D. B. Robinson, *Ind. Eng. Chem. Fundam.* **15**:59 (1976).
7. K. C. Chao and R. L. Robinson, Jr., eds., *Equations of State: Theories and Applications, ACS Symposium Series 300* (Am. Chem. Soc., Washington, DC, 1986).
8. N. F. Carnahan and K. E. Starling, *J. Chem. Phys.* **51**:636 (1969); *AIChE J.* **18**:1184 (1972).
9. C. A. Croxton, *Introduction to Liquid State Physics* (Wiley, London, 1975).
10. R. De Santis, F. Gironi, and L. Marrelli, *Ind. Eng. Chem. Fundam.* **15**:183 (1976).
11. G. Morrison and M. O. McLinden, *NBS Technical Note 1226* (United States Department of Commerce, Washington, DC, 1986).
12. R. Tillner-Roth, *Fundamental Equations of State* (Shaker Verlag, Aachen, 1998).
13. H. C. Longuet-Higgins and B. Widom, *Mol. Phys.* **8**:549 (1964).
14. B. J. Alder and T. E. Wainwright, *J. Chem. Phys.* **27**:1208 (1957); *ibid.* **33**:1439 (1960).
15. J.-P. Hansen and L. Verlet, *Phys. Rev.* **184**:151 (1969).
16. Y. Hiwatari and H. Matsuda, *Progr. Theoret. Phys.* **47**:741 (1972).
17. M. H. Lamm and C. K. Hall, *AIChE J.* **47**:1664 (2001).
18. H. Wenzel and G. Schmit, *Fluid Phase Equilib.* **5**:3 (1980).
19. E. A. Seibold, *Chem. Soc., Farad. Trans. I* **72**:273 (1976).
20. P. H. Salim and M. A. Trebble, *Fluid Phase Equilib.* **93**:75 (1994).
21. R. Span and W. Wagner, *J. Phys. Chem. Ref. Data* **25**:1509 (1996).
22. J. S. Rowlinson and F. L. Swinton, *Liquid and Liquid Mixtures* (Butterworth Scientific, London, 1982).
23. H. G. Donnelly and D. L. Katz, *Ind. Eng. Chem.* **46**:511 (1954).
24. J. A. Davis, N. Rodewald, and F. Kurata, *AIChE J.* **8**:537 (1962).
25. J. O. Hirshfelder, C. F. Curtiss, and R. B. Bird, *Molecular Theory of Gases and Liquids* (Wiley, New York, 1954).
26. U. Setzmann and W. Wagner, *J. Phys. Chem. Ref. Data* **20**:1061 (1991).
27. S. M. Walas, *Phase Equilibria in Chemical Engineering* (Butterworth, Boston, 1985), pp. 54, 58.
28. J. Davalos, W. R. Anderson, R. E. Phelps, and A. J. Kidnay, *J. Chem. Eng. Data* **21**:81 (1976).
29. M. S. Wertheim, *Phys. Rev. Lett.* **10**:321 (1963). E. Thiele, *J. Chem. Phys.* **38**:1959 (1963); *ibid.* **39**:474 (1963).
30. J. G. Kirkwood and E. M. Boggs, *J. Chem. Phys.* **10**:394 (1942).

31. W. W. Wood and J. D. Jacobson, *J. Chem. Phys.* **27**:1207 (1957).

32. W. G. Hoover and F. H. Ree, *J. Chem. Phys.* **49**:3609 (1968).

33. Ch. Tegeler, R. Span, and W. Wagner, *J. Phys. Chem. Ref. Data* **28**:779 (1999).

34. R. C. Reid, J. M. Prausnitz, and B. E. Poling, *The Properties of Gases & Liquids*, 4th ed. (McGraw–Hill, New York, 1987), p. 733.

35. F. H. Ree and W. G. Hoover, *J. Chem. Phys.* **46**:4181 (1967); K. W. Kratky, *J. Statist. Phys.* **29**:129 (1982).

36. E. J. Janse van Rensburg, *J. Phys. A* **26**:4805 (1993).

37. J. G. Loeser, Z. Zhen, S. Kais, and D. R. Herschbach, *J. Chem. Phys.* **95**:4525 (1991).

38. I. C. Sanchez, *J. Chem. Phys.* **101**:7003 (1994).

39. D. A. Kofke, *Ad. Chem. Phys.* **105**:405 (1999); P. A. Monson and D. A. Kofke, *ibid.* **115**:113 (2000).

40. J. H. van der Waals and J. C. Platteeuw, *Adv. Chem. Phys.* **2**:1 (1959).

41. W. R. Parrish and J. M. Prausnitz, *Ind. Eng. Chem. Process Des. Develop.* **11**:26 (1972).

42. P. Pourgheysar, G. A. Mansoori, and H. Modarress, *J. Chem. Phys.* **105**:9580 (1996).

43. W. Wagner, A. Saul, and A. Pruß, *J. Phys. Chem. Ref. Data* **23**:515 (1994).

44. W. G. Hoover and J. C. Poirier, *J. Chem. Phys.* **37**:1041 (1962).

45. A. Jayaraman, R. C. Newton, and J. M. McDonough, *Phys. Rev.* **159**:527 (1967).

46. A. Jayaraman, *Phys. Rev. A* **137**:179 (1965).

47. D. C. Garcia and K. D. Luks, *Fluid Phase Equilib.* **161**:91 (1999).